On Generating Monte Carlo Simulations of Underwater Acoustic Communication Systems with Application to Transmit Beamforming

Denis B. de Souza, Vinicius M. Pinho, Rafael S. Chaves, Marcello L. R. Campos, and José A. Apolinário Jr.

***Abstract*—Underwater Acoustic (UWA) communication systems still rely heavily on at-sea trials. This work presents an operational framework that significantly reduces the need for practical experiments. The key idea is to generate channel impulse responses (CIRs) drawn from probability density functions constructed based on trusted information and to employ Monte Carlo simulations to develop new UWA communication systems. Hence, the proposed operational framework depends only on cheaper-to-acquire physical measurements to produce CIRs. It comprises a model-based CIR replay tool and a stochastic-based UWA channel simulator. The former can be any model-based CIR replay tool, and the latter is proposed in this work and validated using data from four different practical experiments. We also carried out experiments for a transmit beamforming with signals digitally modulated in binary phase-shift keying, which were transmitted by an array and by a single source with equivalent power. For the array, the ideal transmit direction comes from the lowest bit error rate (BER) obtained with computer simulations. This paper compares the performance of the transmit array to the single source transmission and the results of a practical experimental transmission with a Monte Carlo simulation employing the proposed technique. We show that both achieved close results regarding BER and mean squared error. The conclusion is that the proposed operational framework, once adjusted to the specific transmission site, can be used to design new UWA communication systems, eliminating the burden of at-sea trials for tests of new transceivers. Finally, we conducted real-life transmit beamforming experiments to verify the BER gain obtained in practice using the steering angle obtained from simulations.**

***Index Terms*—Channel characterization, channel simulation, Monte Carlo simulation, underwater acoustic communication, stochastic-based simulation, transmit beamforming, transmit arrays, array signal processing, hydrophones, and underwater acoustics projectors.**

I. Introduction

UNDERWATER acoustic communication is firmly rooted in numerous applications. Examples can be found in a plethora of areas, from scientific biological research to commercial oil exploration, including coast defense, marine protection, and climate-change research [1]–[4]. The research on this topic has been driving submarine communication studies further, looking for the best solution for every type of application. Improvements in *underwater acoustic* (UWA) communications depend not only on algorithmic innovations but also on their architectures. In communications, arrays of transmitting and receiving elements provide a way to control the directional properties of transmission and reception. In an underwater environment, UWA arrays are generally used for detection, estimation, and tracking [5]. These arrays form directional beams that enable reliable communication as well as increased transmission gain and range. Recent works have shown that a substantial performance improvement can be achieved by combining beamforming, matched filter, massive MIMO, and simple linear detection schemes, such as *zero-forcing* (ZF) and *minimum mean square error* (MMSE) [6]–[9]. However, unlike *radio-frequency* (RF) communications through the air, whose development is now primarily based on channel-simulation techniques, UWA still relies on extensive sea trials for validation and testing of communication algorithms [10]. This at-sea-trial dependency slows down the progress of new technologies because the required equipment is expensive and not always available.

An alternative to the at-sea-trials is model-based *channel impulse response* (CIR) replay tools, which provide deterministic CIRs based on the ray theory and the environment. Common examples of this type of channel generator are the BELLHOP [11] and TRACEO [12]. The deterministic aspect of this CIRs is a hindrance to the development of reliable UWA communication systems, preventing the use of Monte Carlo simulations. On the other hand, conceiving new modern RF communication systems without employing of Monte Carlo simulations is an arduous task. This simulation technique is vastly used in developing wireless RF systems, providing a way of computing the average behavior of the systems. To overcome the limitations of the model-based CIR replays tools, other works have prosed different approaches.

The authors in [13] have categorized the general methods of simulations. The first group is the direct replay, where the simulator reproduces measured channel conditions [10], [14]. The second group is the stochastic-based replay, in which the simulator generates channel conditions with statistical

Vinicius M. Pinho, Rafael S. Chaves and Marcello L. R. Campos are with the Federal University of Rio de Janeiro (UFRJ) / Alberto Luiz Coimbra Institute for Graduate Studies and Research in Engineering (COPPE) / Signal Multimedia and Telecommunications (SMT), Rio de Janeiro - RJ, Brazil (e-mails: {vinicius.pinho, rafael.chaves, campos}@smt.ufrj.br).

Denis B. de Souza is with the *Instituto de Estudos do Mar Almirante Paulo Moreira* (IEAPM), Rio de Janeiro - RJ, Brazil (e-mail: backer.denis@marinha.mil.br).

José A. Apolinário Jr. is with the Military Institute of Engineering (IME), Rio de Janeiro - RJ, Brazil (e-mail: apolin@ime.eb.br).

The authors are grateful for the financial support provided by CNPq and FINEP (Comunicações Submarinas FINEP-01.13.0421.00).

This study was financed in part by the Coordenação de Aperfeiçoamento de Pessoal de Nível Superior - Brasil (CAPES) - Finance Code 001.

Digital Object Identifier: 10.14209/jcis.2022.19

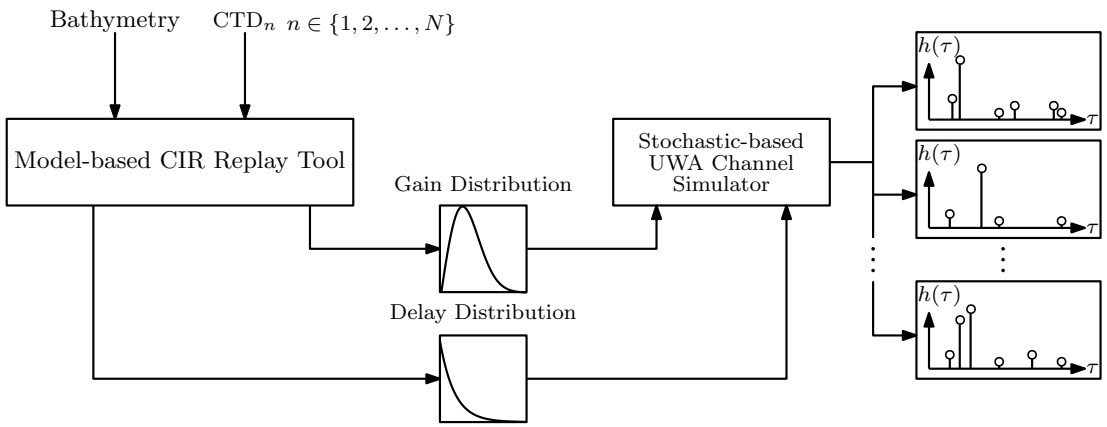

Fig. 1. Operational framework for the novel Monte Carlo UWA channel simulator. CTD stands for conductivity, temperature, and depth.

properties similar to measurements [15]–[17]. However, there is no consensus in the literature for the best *probability density function*s (PDFs) to be used; they vary according to bathymetric profile. Some common distributions are Rayleigh [18], Rice [19], [20], log-normal [21], K [22], and Beta-Nakagami [23]. The third group is the model-based replay, where physical modeling creates the channel conditions based on environmental information [24]–[27]. An interesting approach was recently adopted by [28], in which a ray tracer was extended to incorporate multipath fading, platform mobility effects, and ambient noise. However, the article's purpose is to analyze the acoustic network performance in ice-covered environments, and the validity of the model used in the simulations was not an issue.

The stochastic-based replay is the most suitable option for Monte Carlo simulations, and stochastic-based UWA channel simulators by themselves produce CIRs that can be employed in UWA system simulations. Moreover, it needs to be trustworthy to produce accurate and realistic CIRs that can be used to test UWA communication systems extensively. However, stochastic information about the channel is needed, and this type of data is only acquired from at-sea trials. This paper proposes an alternative to the development of new UWA communication systems, with Monte Carlo simulations based on the operational framework depicted in Fig. 1, where N corresponds to the number of measurements and $h(t)$ a possible CIR.

The main goal of this paper is to propose an operational framework that minimizes the number of at-sea-trials for the development of UWA communications systems. Extensively practical experiments were carried out to validate this proposal. Additionally, the proposed framework is used to investigate a more efficient UWA transmission when an array is employed for transmission. The specific contributions of this paper are:

1) The characterization of the UWA channel of the *Enseada dos Anjos* region, which is a bay in *Arraial do Cabo* in the state of Rio de Janeiro, Brazil ($22°58'38.2''$S, $42°01'10.4''$W). We provide PDFs for the gains and delays for different ranges in the region, which were obtained from numerous practical transmissions. To the best of our knowledge, no other work documents such characterization of this region.
2) An operational framework that ensembles a model-based CIR replay tool and a stochastic-based UWA channel simulator to generate accurate and reliable CIR realizations. The proposed framework minimizes the at-sea-trials by requiring inputs that are cheap to obtain, namely *conductivity, temperature and depth* (CTD) measurements as well as bathymetry. Therefore, the operational framework can output a significant number of CIRs, extending the simulator's capability. Moreover, it will not be necessary to go to sea for further testing once the oceanographic information has been acquired. In order to ensure the reliability of the channel simulator, the statistics of the channels generated by the simulator were compared with real data statistics and confirmed by statistical inference tests. The proposed framework was used to replicate a real at-sea transmission, achieving similar performance as the experiments for *bit-error rate* (BER) and *mean square error* (MSE).
3) A more efficient UWA signal transmission, employing a transmit beamforming. Using a binary phase-shift keying (BPSK) signal and assuming known parameters of the maritime environment, we show how to obtain the beamforming angle that provides the lowest BER compared to the BER resulting from a single source transmitting with equivalent power.

The remaining of this work is organized as follows. Section II presents the general model for the UWA channel and the model used for the transmission when beamforming is employed at the transmitter. Section III characterizes the statistical information of the channel. Section IV shows the process of generating the statistical information to the real channel artificially and validates this data by comparing it with the data obtained from the practical experiments. Section V presents the stochastic-based UWA channel simulator. Section VI shows how the proposed framework functions and how it can be exploited to develop UWA communication systems using Monte Carlo simulations. Section VII presents the transmit beamforming with simulations and experimental results. Finally, the conclusions are drawn in Section VIII.

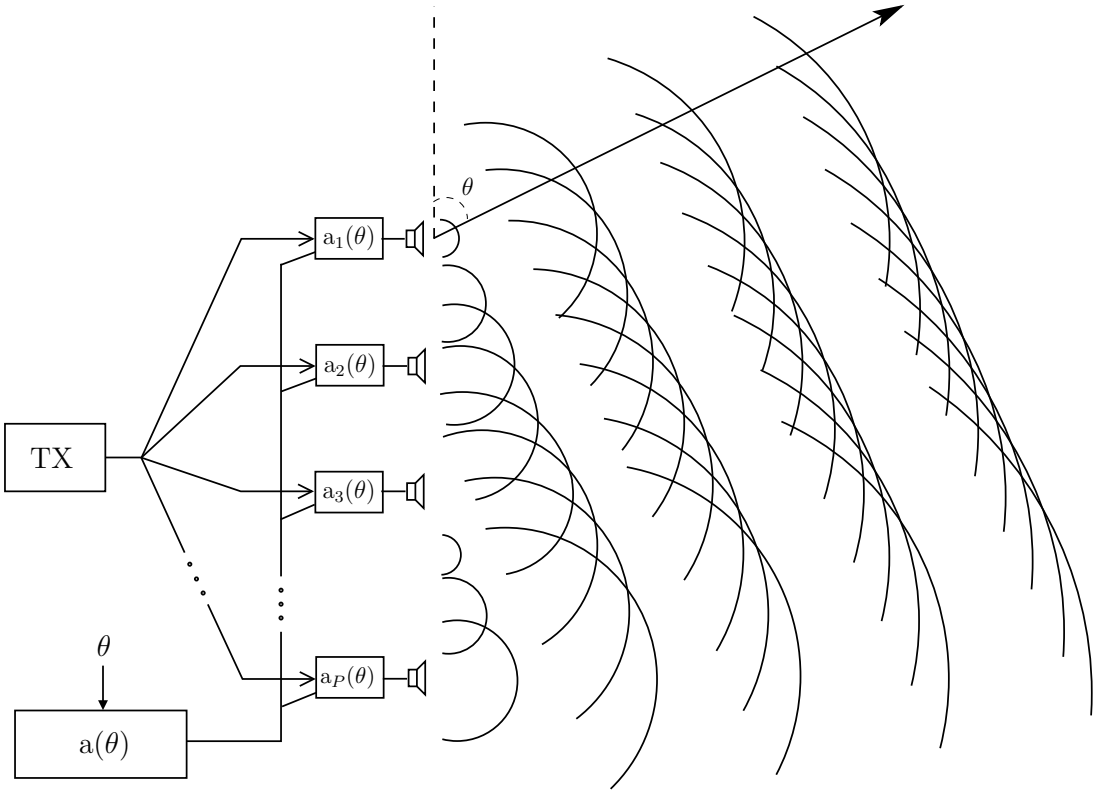

Fig. 2. Sketch of the transmitter with a p-sources array beamforming the transmitted signal at the direction θ.

As for the notation used herein, vectors and matrices are represented in boldface with lowercase and uppercase letters, respectively. The notations $[\cdot]^{\mathrm{T}}$, $[\cdot]^{\mathrm{H}}$, $[\cdot]^{-1}$ stand for transpose, conjugate transpose (Hermitian) and inverse operations on $[\cdot]$, respectively. The symbols $\mathbb{N}$, $\mathbb{R}$, $\mathbb{R}_+$, and $\mathbb{C}$ denote the sets of natural, real, non-negative real, and complex numbers, respectively. The set of $\mathbb{C}^{M\times N}$ denotes all $M \times N$ matrices comprised of complex-valued entries. The operator $\Re\{[\cdot]\}$ stands for the real part of $[\cdot]$. The symbols $\mathbf{0}_{M\times N}$, and $\mathbf{I}_M$ denote an $M \times N$ matrix with zeros and the $M \times M$ identity matrix, respectively.

II. System Model

A. Channel Model

In a typical UWA communication system, the signal transmitted by a source arrives at the receiver through different paths, with distinct directions and delays due to dispersion and reflections in underwater objects, and at the surface and bottom of the sea [29]. These multiple delayed and distorted versions of the transmitted signal can cause *intersymbol interference* (ISI) [30]. Another phenomenon in UWA communication is the Doppler effect due to the ubiquitous relative velocity among the multiple paths between transmitter and receiver. Although Doppler is always present in UWA transmissions since the tide always moves the transmitter and receiver, sometimes it can be neglected, as will be further discussed in Section VI. If we take all these effects into account, we would be able to model the CIR as a linear time-variant system with impulse response given by [31]

$$h(t,\tau) = \sum_{l\in\mathcal{L}} A_l \delta\left(\tau - (\tau_l - a_l t)\right), \tag{1}$$

where $A_l \in \mathbb{R}_+$ is the amplitude for the lth path, $\tau_l(t) \in \mathbb{R}_+$ is the delay for the lth path, a_l is the Doppler scaling factor for the lth path, and $\mathcal{L} = \{1, 2, \cdots, L\}$ is the set containing all path indexes.

B. Transceiver Model

Consider $x(t)$ a narrowband analytical signal given by

$$x(t) = s_n \mathrm{e}^{\mathrm{j}\Omega_0 t}, \tag{2}$$

where, in this work, $s_n \in \mathcal{C} = \{-1, +1\}$ is a BPSK message, $\Omega_0 = 2\pi f_0$ is the angular frequency and $f_0 \in \mathbb{R}_+$ is the carrier frequency. This signal is transmitted by a P-source array, as illustrated in Fig. 2. Each source transmits a delayed version of $x(t)$

$$x_p(t) = x(t - r_p), \tag{3}$$

where $r_p \in \mathbb{R}_+$ is the delay associated with the pth source given by

$$r_p = \frac{d_p \cos(\theta)}{c}, \quad \forall p \in \mathcal{P}, \tag{4}$$

where $\theta \in [0, \pi]$ is the direction of the transmitted signal, $d_p \in \mathbb{R}_+$ is the distance between the pth source and the first source, c is the speed of sound in the environment, and $\mathcal{P} = \{1, 2, \cdots, P\}$ is the set containing all source indexes [32].

Note that $r_1 = 0$ since $d_1 = 0$. The transmitted signal by the pth source can be written as

$$x_p(t) = x(t)\mathrm{e}^{-\mathrm{j}\Omega_0 r_p}, \tag{5}$$

and the transmitted vector $\mathbf{x}(t) = [x_1(t)\ x_2(t)\ \cdots\ x_P(t)]^{\mathrm{T}}$ can be written as

$$\mathbf{x}(t) = x(t)\mathbf{a}(\theta), \tag{6}$$

where $\mathbf{a}(\theta) \in \mathbb{C}^{P\times 1}$ is the steering vector defined as [33]

$$\mathbf{a}(\theta) = \left[1\ \mathrm{e}^{-\mathrm{j}\Omega_0 r_2}\ \cdots\ \mathrm{e}^{-\mathrm{j}\Omega_0 r_P}\right]^{\mathrm{T}}. \tag{7}$$

The received signal $y(t)$ after a transmission with a P-source array through a UWA channel is given by

$$\begin{aligned} y(t) &= \Re\left\{\sum_{p\in\mathcal{P}}\sum_{l\in\mathcal{L}} A_l x_p((1+a_l)t-\tau_l)a_p(\theta)\right\} + w(t), \\ &= \Re\left\{\sum_{p\in\mathcal{P}}\sum_{l\in\mathcal{L}} A_l s_n \mathrm{e}^{\mathrm{j}\Omega_0(1+a_l)t}\mathrm{e}^{-\mathrm{j}\Omega_0\tau_l}a_p(\theta)\right\} + w(t), \end{aligned} \tag{8}$$

where $w(t) \in \mathbb{R}$ is the UWA environment noise. After the modulation and an assumed ideal sampling process, the received signal is given by

$$y_n = \Re\left\{\sum_{p\in\mathcal{P}}\sum_{l\in\mathcal{L}} A_l s_n \mathrm{e}^{\mathrm{j}\Omega_0 a_l n}\mathrm{e}^{-\mathrm{j}\Omega_0\tau_l}a_p(\theta)\right\} + w_n, \tag{9}$$

where w_n is the discrete-time noise and n the discrete time index related to the continuous-time by $t = n/f_s$, f_s doing the sampling frequency.

The performance of this UWA communication system can be evaluated in the terms of the BER. Then, the optimal direction $\theta^\star$ is given by

$$\theta^\star = \min_{\theta\in\mathbb{R}}\{\mathsf{Pr}\left[y_n \neq s_n\right]\}. \tag{10}$$

Finding the optimal direction is an arduous task since the channel is unknown beforehand. An alternative to overcome this issue is using a reliable stochastic-based UWA channel simulator. The following sections present an operational framework that can help with such matters.

We note that underwater acoustics software, using boundary conditions of the wave equation, shows the wave's behavior on the seafloor. However, this tool does not generate a channel impulse response, making it challenging to analyze the received signal, especially for communications with arrays. A channel simulator produces an estimated channel impulse response ($\hat{h}$), which helps identify the signal received after the channel.

III. Statistical Characterization of the Channel

The first step to be considered in the operational framework is to create the model-based CIR replay tool to generate the necessary statistics for a stochastic-based UWA channel simulator validated by real UWA channel experiments. We propose the framework, explain it, and test it using data from *Enseada dos Anjos* ($22°58'38.2''$S, $42°01'10.4''$W). Four practical experiments were carried out to characterize the UWA channel of this area. The statistical characterization consists in providing the PDF for the path gains and delays of the UWA channel of this region.

TABLE I
Setup for the transmissions used in the statistical characterization of the *Enseada dos Anjos*

Experiment	Range (m)	Duration (ms)	
		Chirp	Guard Time
1st	150	240	80
2nd	250	184	92
3rd	1,500	1,000	1,000
4th	250	184	92

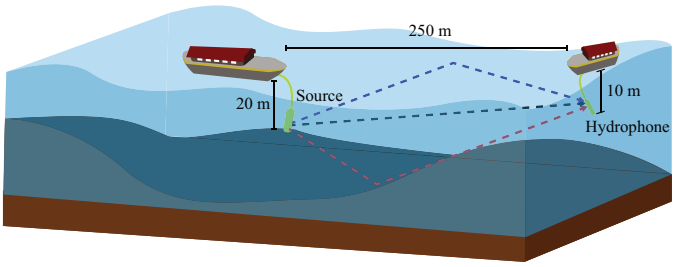

Fig. 3. Illustration of the experiment setup.

Four experimental transmissions were carried out with distinct settings to create diversity in the results. The experiment setups are summarized in Table I. The first two and the fourth trials occurred in the same region at *Enseada dos Anjos*. The first three experiments were intended for channel characterization, and the fourth was to compute the transmission BER used in Section VI.

The experiment setup consisted of a vessel that remained anchored throughout the trial, and it held the transmitter 20 m below the sea surface. The receiver was placed onto the ocean floor close to the shore, at a depth of 10 m, where the seafloor was 20 m deep. The experiment setup is depicted in Fig 3, showing a 250 m transmission range, which is the case for the second and fourth experiments. The distance between the transmitter and the receiver for the first experiment was 150 m. A third practical transmission was carried out outside *Enseada dos Anjos*. Fig. 4 shows the transmitter ($22°58'8.85''$S, $41°58'45.18''$W) and the receiver ($22°58'53.2''$S, $41°59'28.7''$W) locations, 1,500 m apart. As the transmissions have similar structures, a general description is made, and each specificity is explained as needed.

The testbed used for the practical experiments consisted of a transmitter and a receiver with a digital back-end and analog front-end. The digital back-end of the transmitter prepared the signal to be transmitted, which was formed of repeated blocks. The blocks were composed by an up-chirp signal, followed by a guard time employed to avoid interference among blocks – see Table I. Fig. 5 depicts an example of a transmitted block and the corresponding received block in the time and frequency domains. respectively. The analog front-end transmitter received an audio file from the digital back-end transmitter. First, this file was converted into an acoustic

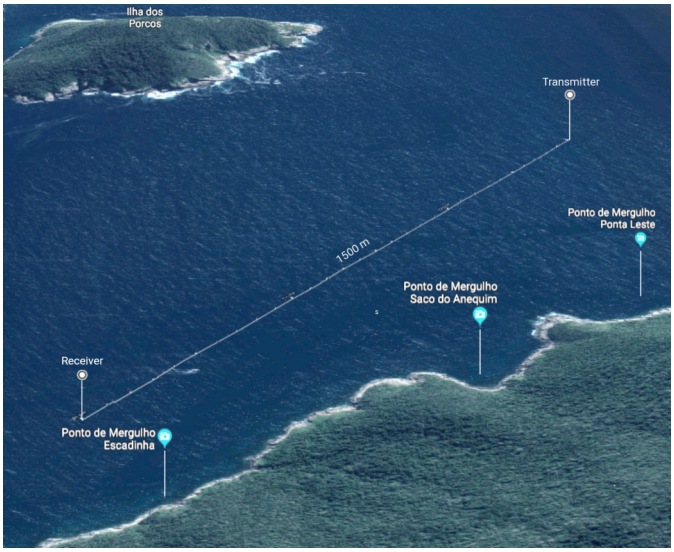

Fig. 4. Transmitter and receiver positions for the 3^{rd} experiment.

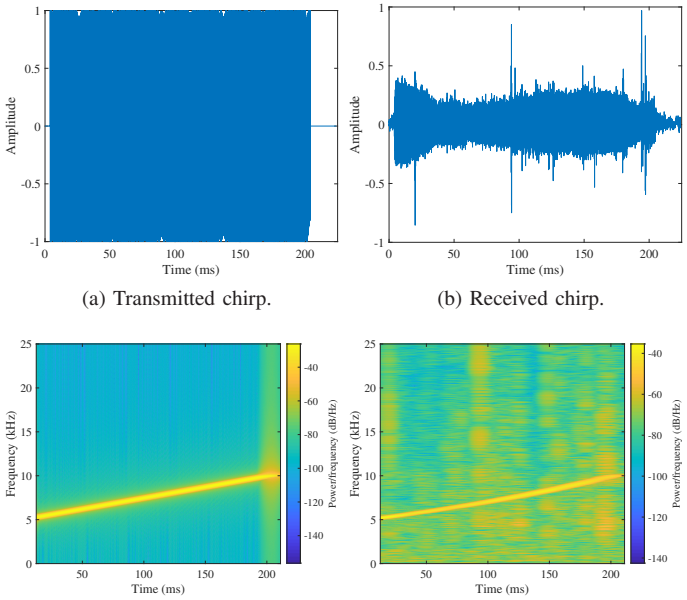

(a) Transmitted chirp. (b) Received chirp.

(c) Transmitted chirp. (d) Received chirp.

Fig. 5. Example of transmitted and received chirp.

signal that was filtered by an analog bandpass filter (5-10 kHz). After this, the resulting signal was transmitted through the UWA channel. At the receiver, the analog front-end converted the received acoustic signal into an audio file sampled with $f_{\mathrm{s}} = 96$ kHz and supplied this file to the digital back-end receiver.

The digital back-end processing part occurred offline. The received signal was filtered by a bandpass filter (5-10 kHz) for mitigating interference from signals outside the frequencies of interest. As the sampling frequency was $f_{\mathrm{s}} = 96$ kHz, the signal was downsampled by a factor $Q = 4$, for better use of computational resources. The result was a sampling frequency $f'_{\mathrm{s}} = 24$ kHz. After filtering and downsampling, the received signal was split into blocks.

Synchronization was indispensable in this experimental system. Each block was treated individually in the digital back-end receiver, so the signal stream had to be correctly split. The synchronization procedure employed a simple cross-correlation between the received signal and the chirp contained in the transmitted signal. Since every block was composed of an up-chirp, the correlation resulted in peaks signaling the beginning of each block. Thus, the block detector divided the signal into blocks, each one containing an up-chirp and a guard time.

The last step in the processing was CIR estimation. To estimate the CIR, the transmission process was modeled as a linear time-invariant system, i.e., the UWA communication system did not consider the Doppler effect. Assuming vector $\boldsymbol{\varphi} \in \mathbb{C}^{N\times 1}$ as the baseband version of the pilot signal, the following equation holds [34]

$$\mathbf{y}_p = \mathbf{H}\boldsymbol{\varphi}, \tag{11}$$

where $\mathbf{y}_p \in \mathbb{C}^{M\times 1}$ is the baseband received pilot, $\mathbf{H} \in \mathbb{C}^{M\times N}$ is the baseband Toeplitz channel matrix, $N \in \mathbb{N}$ is the size of the pilot in samples, and $M \in \mathbb{N}$ is the size of the received pilot in samples. By the linear property of convolution [34], (11) can be rewritten as

$$\mathbf{y}_p = \boldsymbol{\Phi}\mathbf{h}, \tag{12}$$

where $\boldsymbol{\Phi} \in \mathbb{C}^{M\times N}$ is the Toeplitz form of $\boldsymbol{\varphi}$ [35]. Therefore, the least-squares solution of (12) is the estimated CIR

$$\hat{\mathbf{h}} = \left(\boldsymbol{\Phi}^{\mathrm{H}}\boldsymbol{\Phi}\right)^{-1}\boldsymbol{\Phi}^{\mathrm{H}}\mathbf{y}_p. \tag{13}$$

Once the CIR from every transmitted block was estimated, the proposed scheme uses all estimates to compute the statistical information regarding gain and delay distributions.

Fig. 6 shows the histograms of real and imaginary parts of (13) for each experiment. The data obtained from the three experiments pass the Kolmogorov–Smirnov normality test [36], and the number of bins in each histogram follows Scott's rule [37]. The results of these tests indicate that the real and imaginary parts of (13) are Gaussian distributed, i.e., the complex path gains are Rayleigh distributed [38]. Moreover, the delays pass the Kolmogorov–Smirnov test for exponential distribution as in [39]. Similar results regarding the complex path gain distributions were obtained in [17], where experimental shallow water transmissions were carried out in two different sites, in the Atlantic Ocean and the Mediterranean sea, and the Kolmogorov–Smirnov test was also employed. The same results found in shallow water trials in completely different transmission sites help to corroborate our results. These results are standard for RF transmissions, indicating that UWA transmissions in shallow water behave similarly to RF propagation for some specific scenarios.

IV. Artificially Generated UWA Channel Statistics

In this section, a model-based CIR replay tool is used to artificially generate probability distributions similar to the ones

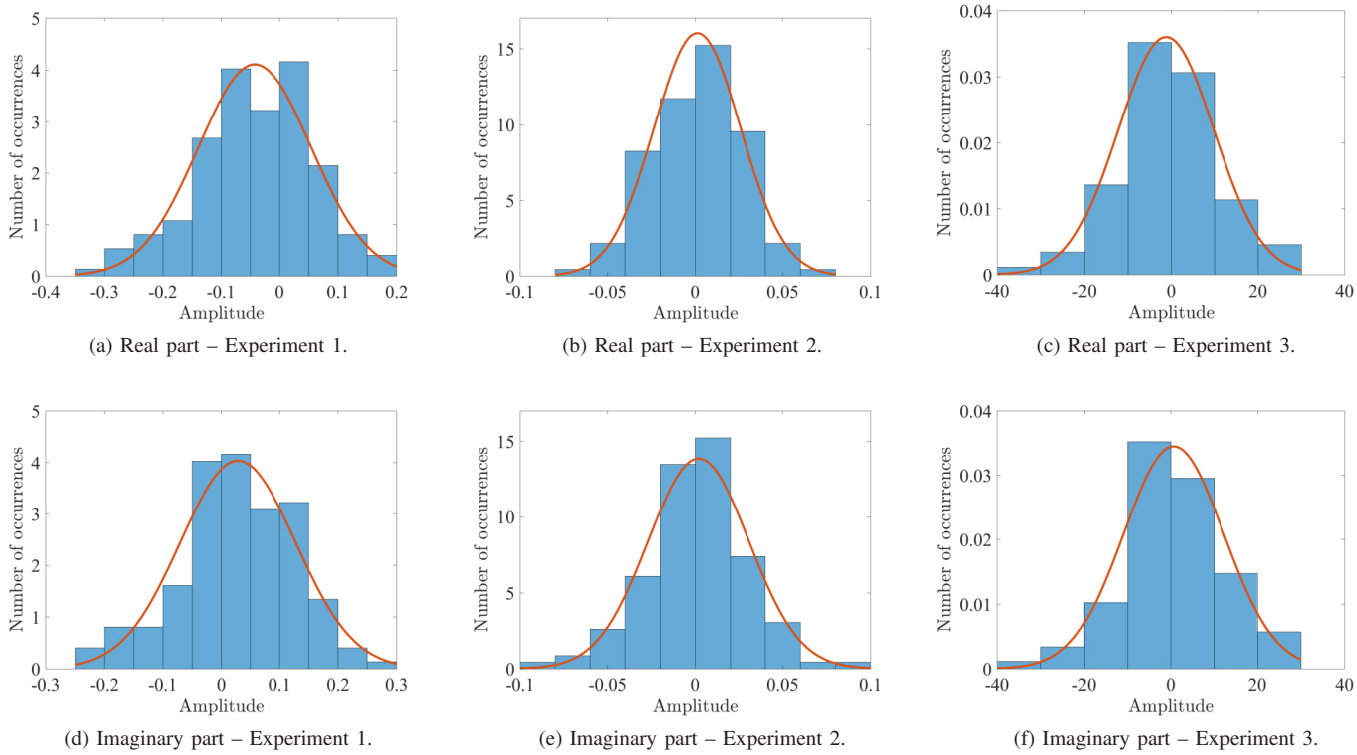

(a) Real part – Experiment 1. (b) Real part – Experiment 2. (c) Real part – Experiment 3.

(d) Imaginary part – Experiment 1. (e) Imaginary part – Experiment 2. (f) Imaginary part – Experiment 3.

Fig. 6. Real and imaginary parts of path gains obtained in the three experiments fitting normal distribution probability density functions.

obtained in Section III. Any model-based CIR replay tool could be used for this task, TRACEO [12] was the one chosen in this paper. TRACEO requires physical parameters of the environment, such as sound speed and bathymetric profiles. The sound speed profile in seawater can be estimated with the Mackenzie equation [40] and CTD data, which shows how the sound speed varies with depth. The bathymetric profile outlines the 2D site in which the transmission is simulated. Considering that the ocean floor does not change significantly over time, a well-depicted bathymetric profile reliably represents the geographic boundaries of the simulation. Fig. 7a and 7b depict an example of a sound speed and the bathymetric profiles of the *Enseada dos Anjos*.

The output of a model-based CIR replay tool only differs (from each other) when the physical parameters change. Since the bathymetric profile can be considered fixed for the area where the experiments took place, different sound speed profiles are used to generate diversity in the CIRs yielded by TRACEO. For each sound speed profile, TRACEO returns the number of different paths received along with each path amplitude, relative delay, and path loss. The path loss indicates the power in dB lost from the transmitter to the receiver. Similarly to the experiments in Section III, all generated CIRs were used to compute statistical data. These statistical data were compared to one obtained from the at-sea experiments in Section III, such as described in Fig. 8. For simplicity and clarity, the remainder of the results compares the distribution obtained with TRACEO and the second practical at-sea experiment setup only. However, similar results were obtained for the other two experiments as well.

Fig. 9 shows the gain distributions obtained in the second practical experiment using TRACEO. Their real and imaginary parts also pass the Kolmogorov–Smirnov test for normality with 5% significance level, indicating the magnitude of the complex gains are Rayleigh distributed. Moreover, as can be observed in the figure, the fitted PDFs are very similar.

Fig. 10 illustrates the delay histograms from the second practical experiment and the model-based CIR replay tool data. They display an exponential behavior, indicated by the red curve used as a reference, and validated using a Kolmogorov–Smirnov test for the exponential distribution as in [39]. As the results show, the gains and delays from the UWA channel of the *Enseada dos Anjos* are circularly Gaussian and exponentially distributed, respectively. Moreover, identical distributions were found with TRACEO when the CTD measurements were used to generate diversity.

V. The Stochastic-based UWA Channel Simulator

The stochastic-based UWA channel simulator is one of the main components of the operational framework, being responsible for receiving the statistical data from the model-based CIR replay tool and for outputting CIRs. [41] introduced the stochastic-based UWA channel simulator presented in this paper, albeit not validated with experimental data. The validation is an important step to verify if the outputs of the simulator correspond to "real" CIRs. The approach to validate the channel simulator is termed *operational validation* [42]. This section presents the stochastic-based UWA channel simulator along with its parameters, characteristics, and validation process.

As the primary intention herein is to accurately represent a UWA channel, the parameters and settings assumed for

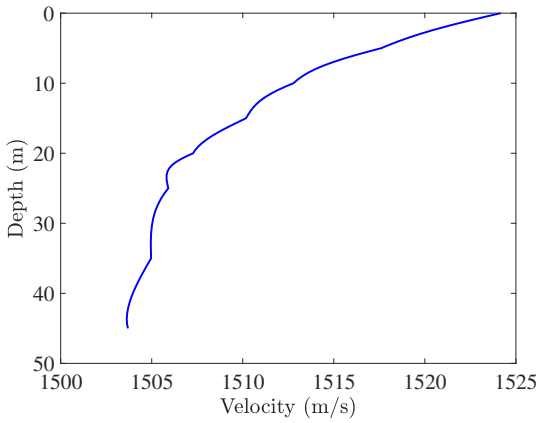

(a) Example of sound speed profile.

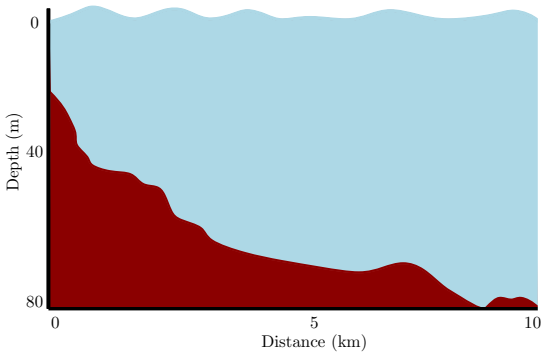

(b) Bathymetric profile of the region.

Fig. 7. Example of physical data from the first and second experiment site, used in the model-based CIR replay tool.

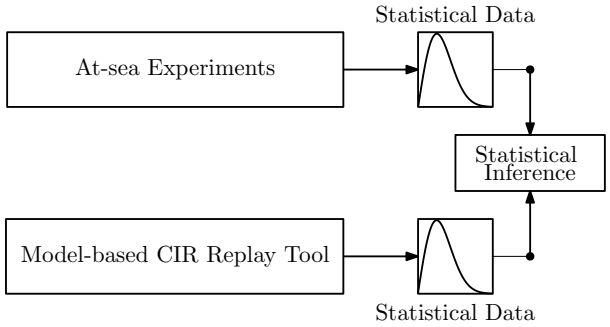

Fig. 8. Framework used for the validation of the distributions obtained with TRACEO.

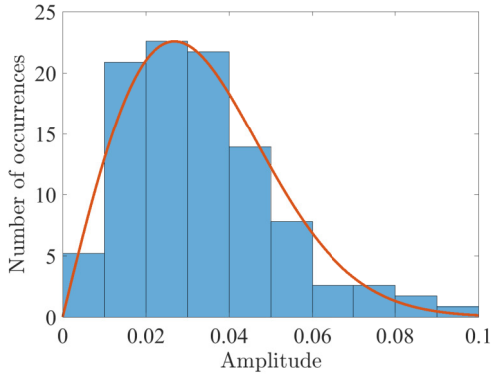

(a) Practical experiment.

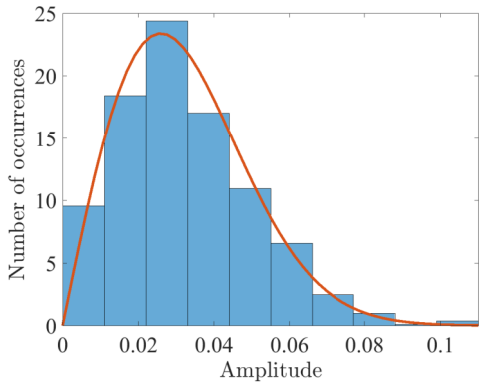

(b) Model-based CIR replay tool.

Fig. 9. Gain histograms following the Rayleigh distribution, data from the second practical experiment settings.

the proposed simulator in this section were verified in experimental transmissions. Although the main output from the channel simulator is the real-valued CIR, the proposed system is also capable of outputting gain and delay separately for each particular path related to the CIR. The simulator requires input parameters, such as the sampling rate, number of paths, delay spread, and attenuation for each path. Moreover, the channel simulator has three options concerning the Doppler effect, allowing to simulate channels considering none, uniform or non-uniform Doppler effect. For uniform Doppler effect, the parameter a_l in (1) is constant for every $l \in \mathcal{L}$. For simulations not considering Doppler effect, the CIR is considered time-invariant, implying in $a_l = 0$. Additionally, the path gains are sorted from a given PDF, which, in this case, is the Rayleigh distribution obtained from the previous section. However, it could be any PDF, depending on the setup to be simulated. Furthermore, parameter τ_l is calculated given the difference between each delay of each path, $\Delta\tau_l$. This parameter, $\Delta\tau_l$, follows an exponential distribution and each τ_l is given by

$$\tau_l = \sum_{i=1}^{l} \Delta\tau_i. \tag{14}$$

In a CIR, for each path, the simulator generates different values of $\Delta\tau_l$ and then uses (14) to compute τ_l. Note that, at least for the *Enseada dos Anjos*, the assumption of exponentially distributed delays was validated by the results obtained in Section III. The following section shows the proposed operational framework in action, comparing the results from an at-sea transmission with simulation using the operational framework.

VI. Operational Framework in Action

The fundamental idea of this paper is to use the operational framework to minimize/remove the need for practical experiments. As depicted in Fig. 1, only CTD measurements, responsible for diversity on the results, and bathymetric profiles are needed to run a model-based CIR replay tool, which is more convenient and cheaper than transmitting signals through the sea. After extracting the statistical information from the

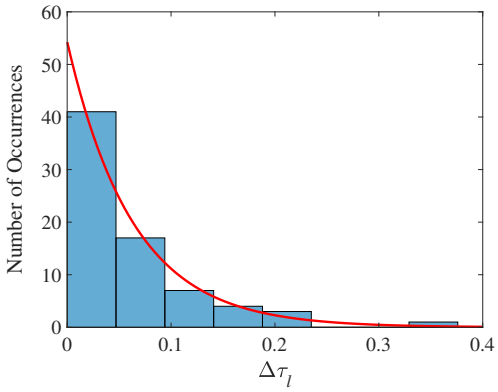

(a) Practical Experiment.

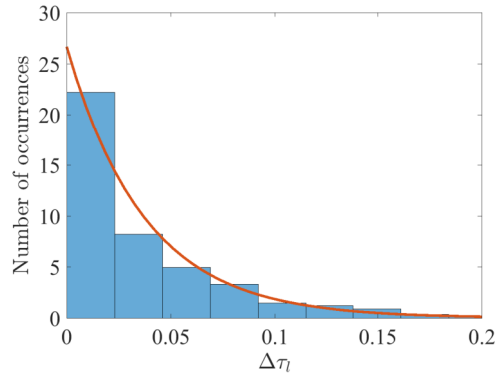

(b) Model-based CIR replay tool.

Fig. 10. Delay distribution following an exponential distribution, data from the practical experiment settings.

model-based CIR replay tool, the proposed simulator runs its stochastic replay, being able to generate a vast number of CIRs. This rapid CIR generation makes the Monte Carlo simulation an attractive and efficient way to obtain diversity within a prescribed valid PDF. In the following, we show the operational framework in action. The goal is to use this framework to reproduce the results from the fourth experimental transmission, which is detailed in [43].

In the experiment, the original message consisted of a ten-by-ten-pixel image. This image was converted into a bitstream, which was encoded by a convolutional code. The trellis structure of the code had a constraint length of 7 and code generator polynomials 171 and 133 (in octal numbers) with a rate of 1/2. The encoded bitstream was modulated by a real-valued *binary phase-shift keying* (BPSK) signal alphabet $\mathcal{C}$. The BPSK-modulated signal was upsampled by a factor $P = \lceil f_s/\mathrm{BW} \rceil$ before going through the TX filter. The TX filter was a lowpass Hamming filter with bandwidth $\mathrm{BW} = 5$ kHz and length 501 that shaped the modulated baseband signal. Moreover, amplitude modulation shifted the baseband signal to $f_c = 7.5$ kHz, generating the passband signal. Then, the message to be transmitted was concatenated with a pilot signal used for synchronization purposes. This pilot consisted of a chirp signal with 184 ms, whose frequency varies linearly from 5 kHz to 10 kHz, plus a guard time of 92 ms.

At the receiver end, the signal was filtered to mitigate interference from signals outside the frequencies of interest. A digital bandpass filter (5-10 kHz) was applied to the signal, and downsampled by a factor $Q = 4$, resulting in a sampling frequency f_s' = 24 kHz. After filtering and downsampling, the received signal was split into blocks. The received message was separated from guard time and chirp within each block. From baseband symbols, the vector was filtered again by a pulse shaping filter and then downsampled again by a factor $P' = \lceil f_s'/\mathrm{BW} \rceil$. The next stage was equalization, where an MMSE equalizer was used, whose coefficients were calculated using the chirp as a training sequence. The equalized signal is demapped into bits and goes into the channel decoder using a soft Viterbi algorithm [44], yielding the estimated transmitted message. Finally, the BER was estimated.

For the simulation, we used a modified version of the UWA transceiver model [43] employed in the practical transmission, as depicted in Fig. 11. The only change from the original model is the introduction of the operational framework from Fig. 1. For the practical transmission, the passband channel block was the sea channel (a real CIR), so the goal was to reproduce this block using the operational framework output.

The first step into the operational framework was the model-based CIR replay tool, which needs bathymetry and CTD data inputs, as detailed in Section IV. By using 731 different CTD measurements collected from the site, we computed the PDFs needed by the stochastic-based UWA channel simulator. As presented in Section V, the inputs to the proposed channel simulator are the sampling rate, the number of paths, delay spread, attenuation for each path, and the gain and delay mean values. After inputting this information, it was possible to generate as many CIRs as desired simply by sampling from the generated PDFs. These characteristics are similar to the real UWA channel, as shown in Section IV. For reproducing the experimental results, $10,000$ CIRs were generated with the stochastic-based UWA channel simulator.

Fig. 12 depicts the BER for both experimental transmission from [43] and simulation, which employed the proposed operational framework. To plot the BER curve *versus* signal-to-noise ratio (SNR) for the experimental data in Fig. 12, white Gaussian noise was added to the received signal in a supervised manner. As observed in the figure, the results obtained through the proposed simulation are very similar to the ones obtained with the experimental data. Moreover, another result that highlights the effectiveness of our proposal is the MSE presented in TABLE II. The differences between MSE values of experimental transmission and simulation are only 0.7 and 0.4 dB for the 5 and 10 dB SNR scenarios, respectively. Furthermore, it is worth highlighting that, when processing the real data, the Doppler effect was not taken into consideration. The results indicated that synchronization and equalization were sufficient to recover a proper version of the transmitted signal. Besides, the stochastic-based UWA channel simulator did not consider the Doppler effect in the simulations, and the similarity between experimental and simulated BER indicates that the Doppler effect was negligible in our experiments.

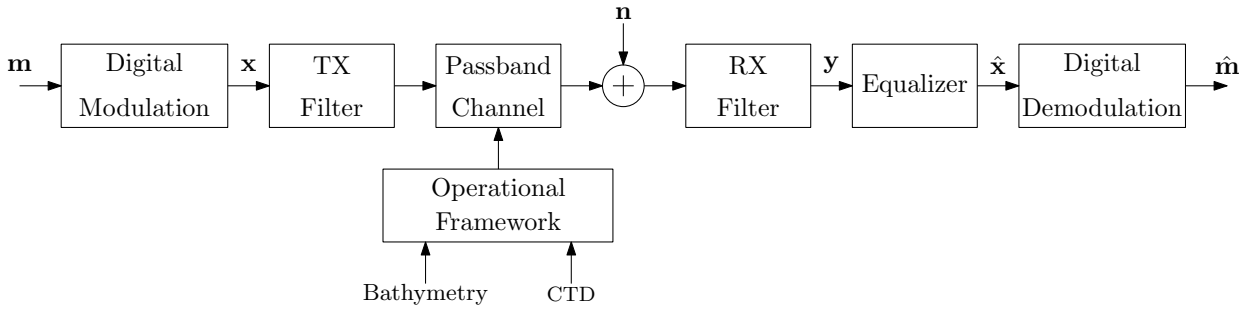

Fig. 11. Baseband model for the UWA transceiver.

TABLE II
MSE BETWEEN TRANSMITTED AND RECEIVED SIGNALS

	MSE (dB)	
Equalizer	SNR = 5 dB	SNR = 10 dB
Experimental	-14.9	-23.7
Simulation	-14.1	-23.3

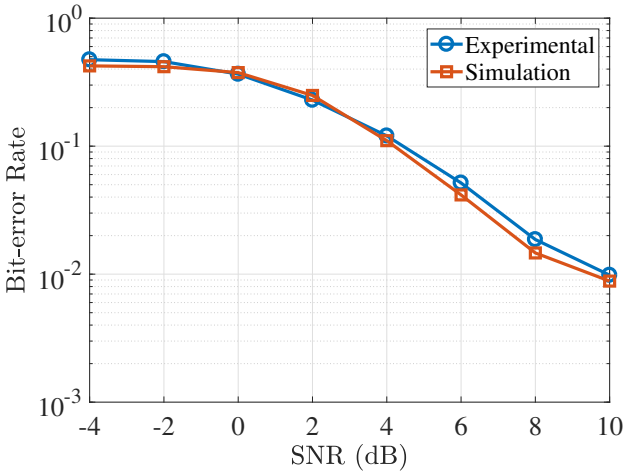

Fig. 12. BER *versus* SNR for the experimental and simulated transmissions.

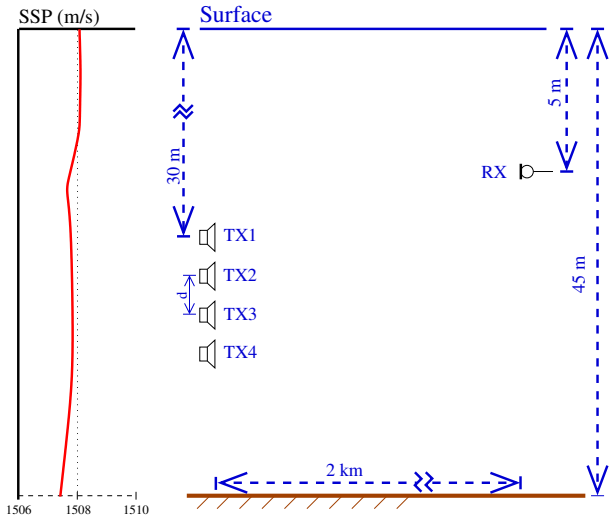

Fig. 13. Illustration of the scenery and sound speed profile of the *Enseada dos Anjos* (provided by IEAPM).

VII. Transmit Beamforming

A. Simulations

The simulations were carried out with a BPSK-modulated signal, a transmission rate of 400 bps, with a message of 100,000 bits, for a linear array of 4 projectors (sources), linearly spaced, d, by 0.12 m, carrier frequency equal to 6,250 Hz, and the steering angle ranging from 0° to 180°, as shown in Fig. 13. The single projector, when used, was placed in the central position of the array (30.18 m deep). Bathymetry and sound speed profiles, in this scenario, were obtained from real data provided by the IEAPM. Through these data, 2,000 CIRs were generated with the stochastic-based UWA channel simulator. The SNR is defined through the singular source with the same power as the transmission beamforming. The measure of communication efficiency employed herein is the BER.

The BER variation is plotted as a function of the steering angle θ for a given SNR, as illustrated in Fig. 14. The SNR in communication with arrays varies according to the beam steering, so the value -7 dB was defined as the SNR of a single source of the same power in the array. Thus, we assumed this amount of noise to be applied in the transmission beamforming for all values of θ. In this case, the noise was generated as white Gaussian noise.

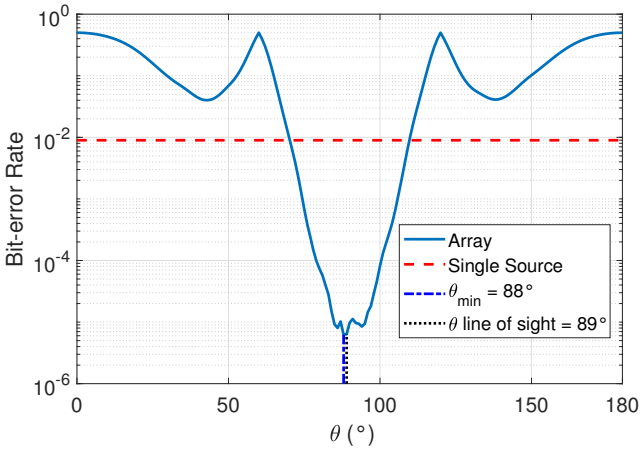

Fig. 14. Graph of the BER as a function of θ. The steering angle = 88° was defined by the smallest BER with SNR equal to -7 dB.

Fig. 15 depicts the BER *versus* SNR, where the SNR ranges from −30 dB to 0 dB with a 2 dB step. As observed in the figure, when a linear array is employed, the BER decreases faster than that with a single source. At -10 dB, the BER reduced from 1.67% to 0.067% when a linear array steered at 88° is employed at the transmitter, yielding a considerable SNR gain of approximately 3.5 dB when compared to a single source transmission.

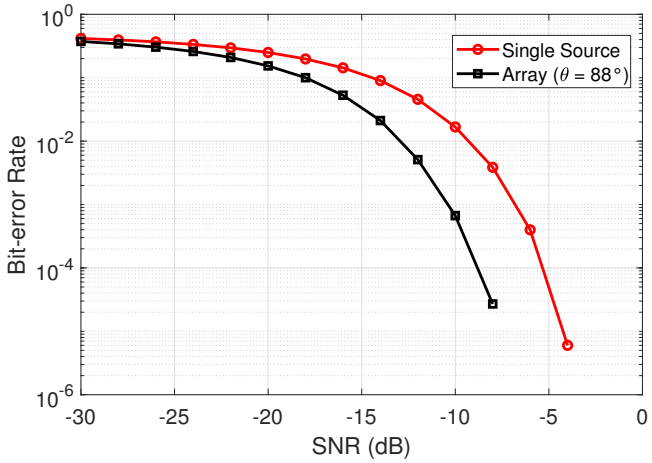

Fig. 15. BER of a singular and array source steered at 88° with SNR varying from -30 dB to 0 dB.

B. Experimental Results

Practical experiments were carried out at *Enseada dos Anjos*, in Arraial do Cabo, Brazil. The linear array (with projectors EDO type "Tonpilz" model 610E) was deployed at a depth of 10 m. The receiver was at a depth of 9 m, with a distance between sensors (transmission and reception) of approximately 500 m. The array's first source was considered the singular source, with twice the gain. The transmitted signals by the array were beamformed between angles 20° and 120°, with a 2°step. The transmitted signal contained 10,000 bits, with a rate of 400 bps and a sampling frequency of 100 kHz. The simulation was performed with 1,000 CIRs generated by the stochastic-based UWA channel simulator.

Fig. 16 shows the BER *versus* θ using the experimental data. Observe, in this figure, a similarity between the curve obtained from the experimental data and the simulated one. The angle that yields the smallest experimental BER is 78°, whereas the simulated one is at 91°. This difference between the experimental and simulated results happens due to different interferences, mainly caused by ambient noise or channel variations, which can cause a false steering angle. However, there is a tendency towards simulated beam steering. Naturally, a smooth curve, possibly close to the simulated curve, would be obtained if we could perform several practical measurements with the same conditions and average the results.

The way to verify the influence of the tide on UWA communication systems was to carry out the same transmission at the beginning and at the end of the experiment, where there was a 40 cm variation in the tide. As can be observed in Fig. 17, there

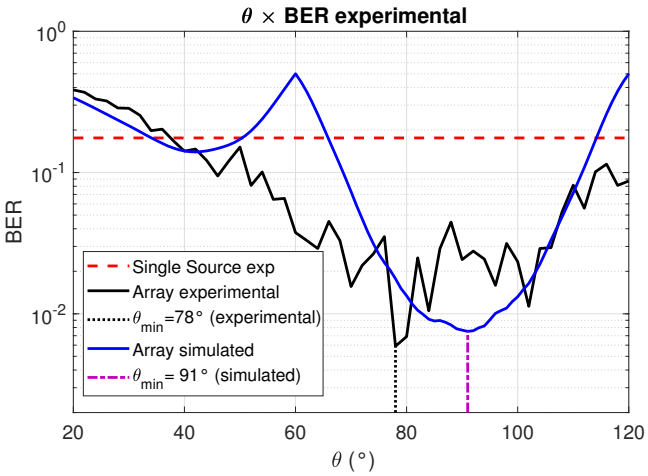

Fig. 16. BER *versus* θ using the experimental data.

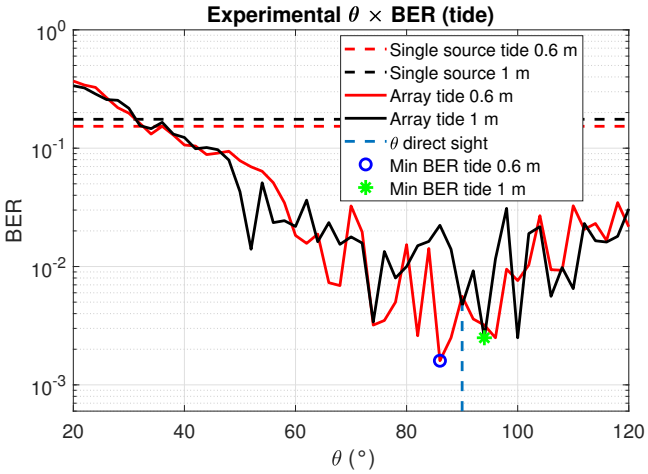

Fig. 17. BER *versus* θ using the experimental data with different tides (0.6 and 1.0 m) and 7.2 dB SNR.

was a difference in the angles of the smallest experimental BER mainly due to tidal variation. The experimental angles were 86° for 0.6 m tide and 94° for 1.0 m tide, which were close to the simulated results where the lowest BER (for both tides) resulted in 91°. Thus, simulated beam steering is a good choice for positioning an experimental transmission with an array.

VIII. Conclusions

In this paper, a novel stochastic-based channel simulator and operational framework for UWA communication were presented and validated. The validation process was done using statistical inference on data from both at-sea experiments and the model-based CIR replay tool, TRACEO. Once validated, the simulator was used to produce CIRs for the proposed operational framework. The operational framework generates CIRs without the need to rely exclusively on at-sea practical transmissions. As shown, the operational framework uses oceanic information, such as bathymetry and CTD, that is to be acquired only once. Then we can produce a significant

number of CIRs that can be used in Monte Carlo simulations. The use of the Monte Carlo simulations reduces the burden of doing at-sea trials for testing a new UWA communication system design, making the development of new technology faster and cheaper. The operational framework was employed in a UWA communication simulation and was compared with practical at-sea experiments with excellent results. This work contributes to guiding the development of UWA communication systems in the direction of using Monte Carlo simulations. Although the channel modeling made in Section V may be simple, the comparison made with the practical experiment showed outstanding results, justifying the use of the chosen model. The take-home message is that it is possible to reproduce the ideas presented in this paper to produce CIR, using CTD and bathymetry as inputs to the operational framework.

With the generation of the channel's impulse response, it was possible to carry out simulations with transmit arrays that presented good results. It was observed that, through a transmission with an array of projectors performing beamforming in a given beam steering, a better result, i.e., reduced BER, is obtained than a single source with equivalent power. The experimental BER graph approached the results obtained by the simulations, mainly the angles of the smallest BER. For the real beam direction to be very close to the estimated one, bathymetry and tidal data must be accurately collected. Another problem that can influence the BER estimation, and consequently, the beam steering, is the time-varying ambient noise that causes variations in the error rates. It was also observed that using the array steered to the angle (θ) of the smallest simulated BER, usually close to the line of sight, was always better than the transmission with a single source. We verified in simulations that the use of the transmission array considerably increases the range of underwater communication.

ACKNOWLEDGMENT

The authors thank Rebeca A. F. Cunha, João P. K. Marques, and Maria L. C. Vianna for their help during the sea experiments and the Brazilian Navy and the IEAPM for the collaboration. The authors also thank Gabriel Chaves for helping with Fig. 3.

REFERENCES

[1] A. A. Myrberg, "Sound Communication and Interception in Fishes," in *Hearing and Sound Communication in Fishes*, W. N. Tavolga, A. N. Popper, and R. R. Fay, Eds. New York, NY, USA: Springer New York, 1981, pp. 395–426, doi: 10.1007/978-1-4615-7186-5.

[2] F. J. L. Ribeiro, A. C. P. Pedroza, and L. H. M. K. Costa, "Underwater Monitoring System for Oil Exploration Using Acoustic Sensor Networks," *Telecommunication Syst.*, vol. 58, no. 1, pp. 91–106, Dec. 2014, doi: 10.1007/s11235-014-9948-6.

[3] M. Matis, "The Protection of Undersea Cables: A Global Security Threat," M.Sc., United States Army War College, Pennsylvania, 2012.

[4] C. Lal, R. Petroccia, M. Conti, and J. a. Alves, "Secure Underwater Acoustic Networks: Current and Future Research Directions," in *IEEE Third Underwater Commun. and Netw. Conf.* Lerici: IEEE, Aug. 2016, pp. 1–5, doi: 10.1109/UComms.2016.7583466.

[5] E. J. Sullivan, *Model-Based Processing for Underwater Acoustic Arrays*, 1st ed. New York, NY, USA: Springer, 2015, doi: 10.1007/978-3-319-17557-7.

[6] L. Liao, Y. V. Zakharov, and P. D. Mitchell, "Underwater Localization Based on Grid Computation and Its Application to Transmit Beamforming in Multiuser UWA Communications," *IEEE Access*, vol. 6, pp. 4297–4307, 2018, doi: 10.1109/ACCESS.2018.2793962.

[7] F. Jiang, C. Li, Z. Gong, Y. Zhang, S. Liu, and K. Hao, "Efficient and Fast Processing of Large Array Signal Detection in Underwater Acoustic Communications," in *IEEE Int. Conf. on Commun.* Shanghai: IEEE, May 2019, pp. 1–6, doi: 10.1109/ICC.2019.8761161.

[8] E. Larsson, F. Tufvesson, O. Edfors, and T. Marzetta, "Massive MIMO for Next Generation Wireless Systems," *IEEE Commun. Mag.*, vol. 52, no. 2, pp. 186–195, Feb. 2014, doi: 10.1109/MCOM.2014.6736761.

[9] F. Jiang, C. Li, and Z. Gong, "Accurate Analytical BER Performance for ZF Receivers Under Imperfect Channel in Low-SNR Region for Large Receiving Antennas," *IEEE Signal Process. Lett.*, vol. 25, no. 8, pp. 1246–1250, Aug. 2018, doi: 10.1109/LSP.2018.2849683.

[10] R. Otnes, P. A. van Walree, and T. Jenserud, "Validation of Replay-Based Underwater Acoustic Communication Channel Simulation," *IEEE J. of Ocean. Eng.*, vol. 38, no. 4, pp. 689–700, Oct. 2013, doi: 10.1109/JOE.2013.2262743.

[11] M. B. Porter, "The BELLHOP manual and User's Guide," HLS Research, User Manual, 2011.

[12] O. R. Camargo, "TRACEO Manual - The ray tracing program," Faculdade de Ciência e Tecnologia, Universidade do Algarve, Algarve, User Manual, 2011.

[13] F.-X. Socheleau, C. Laot, and J.-M. Passerieux, "Parametric Replay-Based Simulation of Underwater Acoustic Communication Channels," *IEEE J. of Ocean. Eng.*, vol. 40, no. 4, pp. 796–806, Oct. 2015, doi: 10.1109/JOE.2015.2458211.

[14] P. van Walree, T. Jenserud, and M. Smedsrud, "A Discrete-Time Channel Simulator Driven by Measured Scattering Functions," *IEEE J. on Sel. Areas in Commun.*, vol. 26, no. 9, pp. 1628–1637, Dec. 2008, doi: 10.1109/JSAC.2008.081203.

[15] P. Qarabaqi and M. Stojanovic, "Statistical Characterization and Computationally Efficient Modeling of a Class of Underwater Acoustic Communication Channels," *IEEE J. of Ocean. Eng.*, vol. 38, no. 4, pp. 701–717, Oct. 2013, doi: 10.1109/JOE.2013.2278787.

[16] R. Galvin and R. E. W. Coats, "A Stochastic Underwater Acoustic Channel Model," in *OCEANS 96 MTS/IEEE Conf. Proc. The Coastal Ocean - Prospects for the 21st Century*. Fort Lauderdale: IEEE, Sep. 1996, pp. 203–210, doi: 10.1109/OCEANS.1996.572599.

[17] F. X. Socheleau, C. Laot, and J. M. Passerieux, "Stochastic Replay of Non-WSSUS Underwater Acoustic Communication Channels Recorded at Sea," *IEEE Trans. on Signal Process.*, vol. 59, no. 10, pp. 4838–4849, Jun. 2011, doi: 10.1109/TSP.2011.2160057.

[18] M. Chitre, "A High-frequency Warm Shallow Water Acoustic Communications Channel Model and Measurements," *The J. of the Acoustical Soc. of America*, vol. 122, no. 5, pp. 2580–2586, Aug. 2007, doi: 10.1121/1.2782884.

[19] A. Radosevic, J. G. Proakis, and M. Stojanovic, "Statistical Characterization and Capacity of Shallow Water Acoustic Channels," in *OCEANS 2009-EUROPE*. Bremen: IEEE, May 2009, pp. 1–8, doi: 10.1109/OCEANSE.2009.5278349.

[20] N. Bahrami, N. H. H. Khamis, and A. B. Baharom, "Study of Underwater Channel Estimation Based on Different Node Placement in Shallow Water," *IEEE Sensors J.*, vol. 16, no. 4, pp. 1095–1102, Feb. 2016, doi: 10.1109/JSEN.2015.2493102.

[21] B. Tomasi, P. Casari, L. Badia, and M. Zorzi, "A Study of Incremental Redundancy Hybrid ARQ over Markov Channel Models Derived from Experimental Data," in *Fifth ACM Int. Workshop on Underwater Networks*. New York, NY, USA: ACM Press, Sep. 2010, pp. 1–8, doi: 10.1145/1868812.1868816.

[22] W.-B. Yang and T. C. Yang, "High-Frequency Channel Characterization for M-ary Frequency-Shift-Keying Underwater Acoustic Communications," *The J. of the Acoustical Soc. of America*, vol. 120, no. 5, p. 2615, Nov. 2006, doi: 10.1121/1.2346133.

[23] H. Kulhandjian and T. Melodia, "Modeling Underwater Acoustic Channels in Short-Range Shallow Water Environments," in *Proc. of the Int. Conf. on Underwater Networks Syst.* New York, NY, USA: ACM Press, Nov. 2014, pp. 1–5, doi: 10.1145/2671490.2674560.

[24] B. Blankenagel and A. G. Zajic, "Simulation Model for Wideband Mobile-to-Mobile Underwater Fading Channels," in *IEEE 77th Veh Technol. Conf.* Dresden: IEEE, Jun. 2013, pp. 1–5, doi: 10.1109/VTC-Spring.2013.6692754.

[25] A. G. Zajic, "Statistical Modeling of Underwater Wireless Channels," in *IEEE Global Telecommun. Conf.* Miami, FL, USA: IEEE, Dec. 2010, pp. 1–5, doi: 10.1109/GLOCOM.2010.5683602.

[26] L. M. Wolff, E. Szczepanski, and S. Badri-Hoeher, "Acoustic Underwater Channel and Network Simulator," in *2012 Oceans - Yeosu*. Yeosu: IEEE, May 2012, pp. 1–6, doi: 10.1109/OCEANS-Yeosu.2012.6263608.
[27] A. G. Zajic, "Statistical Modeling of MIMO Mobile-to-Mobile Underwater Channels," *IEEE Trans. on Veh. Technol.*, vol. 60, no. 4, pp. 1337–1351, May 2011, doi: 10.1109/TVT.2011.2129603.
[28] K. Pelekanakis, R. Petroccia, Y. Fountzoulas, D. Green, S. Fioravanti, J. Alves, S. Blouin, and S. Pecknold, "A simulation study for long-range underwater acoustic networks in the high north," *IEEE J. of Ocean. Eng.*, vol. 44, no. 4, pp. 850–864, 2019, doi: 10.1109/JOE.2019.2931853.
[29] X. Lurton, *An Introduction to Underwater Acoustics: Principles and Applications*, 2nd ed. Praxis Berlin, 2010. ISBN 978-3-662-49969-6
[30] R. S. H. Istepanian and M. Stojanovic, *Underwater Acoustic Digital Signal Processing and Communication Systems*, 1st ed. Boston, MA, USA: Springer US, 2002, doi: 10.1007/978-1-4757-3617-5.
[31] S. Zhou and Z. Wang, *OFDM for Underwater Acoustic Communications*, 1st ed. Chichester: John Wiley & Sons, Ltd, 2014, doi: 10.1002/9781118693865.
[32] D. B. de Souza, J. A. Apolinário Jr., and M. L. R. Campos, "Uma Proposta de Beamforming de Transmissão para Sinais Subaquáticos (in portuguese)," in *XXXVII Brazilian Telecommun. Symp. (SBrT'19)*, Petrópolis, Oct. 2019, pp. 1–5, doi: 10.14209/sbrt.2019.1570558587.
[33] H. L. van Trees, *Optimum Array Processing*, 1st ed. New York, NY, USA: John Wiley & Sons, Inc., 2002, doi: 10.1002/0471221104.
[34] C. Chen, *Linear System Theory and Design*, ser. The Oxford Ser. in Elect. and Comput. Eng. Oxford University Press, 2014. ISBN 9780199964543
[35] H. Anton, C. Rorres, and A. Kaul, *Elementary Linear Algebra: Applications Version*, 12th ed. Wiley, 2019. ISBN 978-1-119-28236-5
[36] H. W. Lilliefors, "On the Kolmogorov-Smirnov Test for Normality with Mean and Variance Unknown," *J. of the American Statistical Assoc.*, vol. 62, no. 318, pp. 399–402, Jun. 1967, doi: 10.2307/2283970.
[37] D. W. Scott, "Scott's Rule," *Wiley Interdisciplinary Reviews: Comput. Statist.*, vol. 2, no. 4, pp. 497–502, Jul. 2010, doi: 10.1002/wics.103.
[38] P. Z. Peebles, *Probability, Random Variables And Random Signal Principles*, 4th ed. New York, NY, USA: McGraw-Hill, 2002. ISBN 0073660078
[39] H. W. Lilliefors, "On the Kolmogorov-Smirnov Test for the Exponential Distribution with Mean Unknown," *J. of the American Statistical Assoc.*, vol. 64, no. 325, pp. 387–389, Mar. 1969, doi: 10.2307/2283748.
[40] K. V. Mackenzie, "Nine-Term Equation for Sound Speed in the Oceans," *The J. of the Acoustical Soc. of America*, vol. 70, no. 3, pp. 807–812, Sep. 1981, doi: 10.1121/1.386920.
[41] R. S. Chaves, W. A. Martins, and P. S. R. Diniz, "Modeling and Simulation of Underwater Acoustic Communication Systems," in *XXXV Brazilian Telecommun. Symp. (SBrT'17)*. São Pedro: SBrT, Sep., pp. 607–611, doi: 10.14209/sbrt.2017.218.
[42] R. G. Sargent, "Verification and Validation of Simulation Models," *J. of Simul.*, vol. 7, no. 1, pp. 12–24, Feb. 2013, doi: 10.1109/WSC.2010.5679166.
[43] V. M. Pinho, R. S. Chaves, and M. L. R. Campos, "On Equalization Performance in Underwater Acoustic Communication," in *XXXVI Brazilian Telecommun. Symp. (SBrT'18)*, Campina Grande, Jul. 2018, doi: 10.14209/sbrt.2018.207.
[44] J. G. Proakis and M. Salehi, *Digital Communications*, 5th ed. New York, NY, USA: McGraw-Hill Education, 2007. ISBN 0072957166

Denis B. de Souza was born in Rio de Janeiro, Brazil, in 1977. He graduated in Electrical Engineering with an emphasis on electrical energy systems from the Pontifical Catholic University of Rio de Janeiro, PUC-Rio, in 2005. He received an M.Sc. degree in Defense Engineering from the Military Institute of Engineering, IME. Denis is a member of the Brazilian Navy and serves as Lieutenant Commander in the Underwater Acoustics Department of the IEAPM.

Vinicius M. de Pinho was born in Cachoeiro de Itapemirim, Brazil, in 1995. He received the Electronics and Computing Engineering degree from the Polytechnic School/UFRJ in 2018 and his M.Sc. degree in Electrical Engineering from Instituto Alberto Luiz Coimbra de Pós-Graduação e Pesquisa de Engenharia (COPPE), in 2021. Vinicius is currently an Early Stage Researcher at Nokia Bell Labs, working on the PAINLESS project within the framework of the H2020 Marie Skłodowska-Curie Innovative Training Networks.

Rafael S. Chaves was born in Rio de Janeiro, Brazil, in 1992. He received the Electronics and Computing Engineering degree from the Polytechnic School, Federal University of Rio de Janeiro (UFRJ) in 2016 when he was awarded the best undergraduate student of that year. In 2018, he received an M.Sc. degree in Electrical Engineering from COPPE/UFRJ. He is pursuing his cotutelle Ph.D. degree with COPPE/UFRJ and School of Engineering, Macquarie University, Sydney, Australia. He is a member of the IEEE and the Brazilian Telecommunications Society (SBrT). His research interests include digital signal processing, adaptive signal processing, tensor signal processing, wireless communications, massive MIMO systems, underwater acoustic communications, and machine learning.

Marcello L. R. de Campos was born in Niteroi, Brazil, in 1968. He received the Engineering (*cum laude*) degree from the Federal University of Rio de Janeiro (UFRJ), Rio de Janeiro, Brazil, in 1990, the M.Sc. degree from COPPE/UFRJ in 1991, and the Ph.D. degree from the University of Victoria, Victoria, BC, Canada, in 1995, all in Electrical Engineering. In 1996, he was a Post-Doctoral Fellow with the Department of Electronics, School of Engineering, UFRJ, and with the Program of Electrical Engineering, COPPE/UFRJ. From 1997 until 1998, he was an Associate Professor with the Department of Electrical Engineering, Military Institute of Engineering, Rio de Janeiro. Since 1998 he has been with the Electrical Engineering Program, COPPE/UFRJ, having served as Vice-Chair and Chair in 2004 and 2005, respectively. He is currently a Full Professor and Academic Director for COPPE, serving a four-year term ending in 2023. In 1998, he was with the Laboratory for Telecommunications Technology, Helsinki University of Technology, Espoo, Finland. In 2001, he received a Nokia Visiting Fellowship to visit the Center for Wireless Communications, University of Oulu, Oulu, Finland. In 2008, he visited Unik, the University Graduate Center of the University of Oslo, Oslo, Norway. In 2016, he visited Aalto University, Helsinki, Finland, as part of the mobility program for the Smart2 project, Erasmus Mundus Program, and in 2018 he visited the National University of Science and Technology, Norway, for a micro-sabbatical. He has taught over 150 courses on mobile communications in 15 countries. His research interests include adaptive signal processing in general and its application to distributed networks, in particular, adaptive beamforming, statistical signal processing, signal processing for communications, underwater, mobile, and wireless communications, and MIMO systems. He served as the IEEE Communications Society Regional Director for Latin America in 2000 and 2001, Local-Arrangements Co-Chair for GLOBECOM99, Finance Chair for SPAWC 2008, Plenary Chair for ISCAS 2011, and Technical Co-Chair for the 2013 Brazilian Telecommunications Symposium. He founded and was Chair of the IEEE Signal Processing Society Rio de Janeiro Chapter from 2011 to 2017.

José A. Apolinário Jr. : graduated from the Military Academy of Agulhas Negras (AMAN), Brazil, in 1981 and received the B.Sc. degree from the Military Institute of Engineering (IME), Brazil, in 1988, the M.Sc. degree from the University of Brasília (UnB), Brazil, in 1993, and the D.Sc. Degree from the Federal University of Rio de Janeiro (COPPE/UFRJ), Rio de Janeiro, Brazil, in 1998, all in electrical engineering. He is currently an Associate Professor with the Department of Electrical Engineering, IME, where he has already served as Head of the Department and as Vice-Rector for Study and Research. He was a Visiting Professor at the Escuela Politécnica del Ejército (ESPE), Quito, Ecuador, from 1999 to 2000, and a Visiting Researcher and twice a Visiting Professor at Helsinki University of Technology (HUT, today Aalto University), Finland, in 1997, 2004, and 2006, respectively. His research interests comprise many aspects of digital signal processing, including adaptive filtering, speech and audio processing, emitter localization, and array signal processing. Dr. Apolinário has organized and been the first Chair of the Rio de Janeiro Chapter of the IEEE Communications Society. He has edited the book "QRDRLS Adaptive Filtering" (Springer, 2009) and served as the Finance Chair of IEEE ISCAS 2011 (Rio de Janeiro, Brazil, May 2011). Dr. Apolinário is a senior member of the IEEE and a senior member of the Brazilian Telecommunications Society (SBrT).